Biochemical and Biophysical Research Communications 443 (2014) 1105–1109

Contents lists available at ScienceDirect

Biochemical and Biophysical Research Communications

journal homepage: www.elsevier.com/locate/ybbrc

CDK inhibitors, p21^{Cip1} and p27^{Kip1}, participate in cell cycle exit of mammalian cardiomyocytes

Shoji Tane [a], Aiko Ikenishi [a], Hitomi Okayama [a], Noriko Iwamoto [a,1], Keiichi I. Nakayama [b], Takashi Takeuchi [a,*]

[a] School of Life Sciences, Faculty of Medicine, Tottori University, Yonago 683-8503, Japan
[b] Medical Institute of Bioregulation, Kyushu University, Fukuoka 812-8582, Japan

ARTICLE INFO

Article history:
Received 16 December 2013
Available online 28 December 2013

Keywords:
CDK inhibitor
Cell cycle exit
Cardiomyocyte
Mouse

ABSTRACT

Mammalian cardiomyocytes actively proliferate during embryonic stages, following which cardiomyocytes exit their cell cycle after birth. The irreversible cell cycle exit inhibits cardiac regeneration by the proliferation of pre-existing cardiomyocytes. Exactly how the cell cycle exit occurs remains largely unknown. Previously, we showed that cyclin E- and cyclin A-CDK activities are inhibited before the CDKs levels decrease in postnatal stages. This result suggests that factors such as CDK inhibitors (CKIs) inhibit CDK activities, and contribute to the cell cycle exit. In the present study, we focused on a Cip/Kip family, which can inhibit cyclin E- and cyclin A-CDK activities. Expression of p21^{Cip1} and p27^{Kip1} but not p57^{Kip2} showed a peak around postnatal day 5, when cyclin E- and cyclin A-CDK activities start to decrease. p21^{Cip1} and p27^{Kip1} bound to cyclin E, cyclin A and CDK2 at postnatal stages. Cell cycle distribution patterns of postnatal cardiomyocytes in *p21^{Cip1}* and *p27^{Kip1}* knockout mice showed failure in the cell cycle exit at G1-phase, and endoreplication. These results indicate that p21^{Cip1} and p27^{Kip} play important roles in the cell cycle exit of postnatal cardiomyocytes.

© 2013 Elsevier Inc. All rights reserved.

1. Introduction

In mammals, cell proliferation and hypertrophy in cardiomyocytes increase the size of the heart before and after birth, respectively. The regulation of proliferation in cardiomyocytes is important during development and the adult stage because it is required for normal morphogenesis, determines the appropriate heart size, and maintains heart function.

Proliferation levels of mouse cardiomyocytes (CMs) are high during early embryogenesis and start to decrease around embryonic day 10–12 (E10–12) [1,2]. Eighty to ninety percent of CMs become binucleated cells during the first 2 weeks after birth [3,4]. Subsequently, both mono- and binucleated CMs exit their cell cycles. Recent studies have shown that postnatal CMs reenter the cell cycle in normal mammals [5,6]. However, the percentages are extremely low (at most, 0.007–0.015% in adult mice) [6]. Therefore, the cell cycle exit is maintained in almost all CMs. The cell cycle exit inhibits cardiac regeneration via the proliferation of pre-existing cardiomyocytes. It remains largely unknown how the cell cycle exit is caused and maintained.

Analysis of cell cycle in the heart showed that the mitotic indices in CMs, and the expression and activation levels of main cyclin-CDK complexes (cyclin D-CDK4/6, cyclin E-CDK2, cyclin A-CDK1/2 and cyclin B-CDK1) in the hearts are high during early embryonic stages. These levels decrease from midgestation to birth, and then show one wave in which the peak is around postnatal day 5 (P5) [1–4]. The wave mainly produces binucleated cells from mononucleated cells. Then, all expression and activation levels of main cyclin-CDK complexes become extremely low or undetectable after P14, and the levels are maintained for life [4]. Our detailed analysis of cyclin E-CDK and cyclin A-CDK complexes showed that these CDK activities decrease significantly after P5, while the CDK levels decrease significantly after P10 [4]. This result suggests that factors such as CDK inhibitors (CKIs) inhibit CDK activity, and contribute to the cell cycle exit.

CKIs are classified into two groups, the INK4 and Cip/Kip families. INK4 family members bind only to CDK4/6 and inhibit their activities, however, Cip/Kip family members can inhibit the activities of cyclin E- and A-CDKs [7]. Therefore, we focused on the Cip/Kip family as potent inhibitors in CMs during postnatal stages. No apparent abnormalities have been reported in the hearts of

Abbreviations: CM, cardiomyocyte; CDK, cyclin dependent kinase; CKI, cyclin dependent kinase inhibitor; KO, knockout.

* Corresponding author. Address: Division of Biosignaling, Department of Biomedical Sciences, School of Life Sciences, Faculty of Medicine, Tottori University, 86 Nishicho, Yonago, Tottori 683-8503, Japan. Fax: +81 859 38 6233.
E-mail address: takeuchi@med.tottori-u.ac.jp (T. Takeuchi).
[1] Present address: Kinutani Women's Clinic, Hiroshima 730-0035, Japan.

0006-291X/$ - see front matter © 2013 Elsevier Inc. All rights reserved.
http://dx.doi.org/10.1016/j.bbrc.2013.12.109

mice deficient in Cip/Kip genes [8–13]. However, detailed analyses of the hearts, especially the cell cycle in CMs, have not been reported.

In the present study, we examined carefully the cell cycle distribution patterns of postnatal CMs in Cip/Kip knockout (KO) mice. Here, we describe the phenotypes in cell cycle exit, and report that $p21^{Cip1}$ and $p27^{Kip}$ play important roles in cell cycle exit of postnatal CMs.

2. Materials and methods

2.1. Mice

Mice with C57BL/6 Jcl (Clea Japan) genetic backgrounds were used. *$p21^{Cip1}$* KO (a kind gift from Dr. Leder, Harvard University, USA) and *$p27^{Kip1}$* KO mice were used in this study [8,11]. The presence of a vaginal plug was regarded as embryonic day 0.5 (E0.5). All mice were genotyped by PCR. All animals were handled and maintained in accordance with institutional guidelines (Animal Care and Use Committee, Tottori University) and the Guidelines for Proper Conduct of Animal Experiments (Science Council of Japan).

2.2. Enzymatic dissociation of CMs into single cells and measurement of DNA content on slide glasses

Enzymatic dissociation of CMs of the cardiac ventricles into single cells was performed as described previously [4,14]. Dissociated CMs were fixed with 4% paraformaldehyde at 4 °C for 24 h. The CMs were washed once with distilled water and then smeared on slide glasses. CMs were identified by staining with an antibody to α-sarcomeric actin (Table 1), as described in histological methods [15]. Cells in the M-phase were stained with an antibody against phospho-histone H3-Ser10 (pH3-S10. Table 1). DNA was stained with 1 μg/ml DAPI for 30 min. After staining, fluorescence images were acquired with microscopes (BZ-9000, Keyence) equipped with imaging software (Viewer BZ-II, Keyence) at room temperature. A microscopy camera in BZ-9000 was used. Then DNA content per nucleus of CMs was measured with a Cell Cycle Application Module of MetaMorph software (Molecular Devices). Mono- and binucleated CMs were identified by observation, and their cell cycle distribution patterns were analyzed independently. Approximately 340–480 and 70–160 nuclei of bi- and mononucleated CMs, respectively, were analyzed per mouse.

2.3. Western blot analysis and immunoprecipitation

The cardiac ventricles were lysed and then immunoprecipitation, Western blot analysis were performed as described previously [2,4,15,16]. Antibodies used for immunoprecipitation and Western blot analysis are shown in Table 1.

Table 1
Antibodies used in this study.

Antigens	Antibodies	Assays
Cyclin E	07-683; Millipore Co.	WB
Cyclin A	CY-A1; Sigma Chemical Co.	WB
Cyclin B1	V152; Cell Signaling Technology	WB
CDK2	sc-163; Santa Cruz Biotechnology Inc.	WB, IP
CDK1	sc-54; Santa Cruz Biotechnology Inc.	WB
$p21^{Cip1}$	SX118; BD Parmingen	WB, IP
$p27^{Kip1}$	G173-524; BD Parmingen	WB, IP
$p57^{Kip2}$	P0357; Sigma Chemical Co.	WB
GAPDH	sc-32233; Santa Cruz Biotechnology Inc.	WB
pH3-S10	06-570; Millipore Co.	IF
α-Sarcomeric actin	5C5; Sigma Chemical Co.	IF

WB; Western blotting, IP; Immunoprecipitation, IF; Immunofluorescence.

2.4. Statistical analysis

The experimental data were analyzed using Student's *t* test.

3. Results

3.1. Expression patterns and complex formation of Cip/Kip family proteins

We examined the expression patterns of Cip/Kip family in cardiac development. Expression of $p21^{Cip1}$ and $p27^{Kip1}$ after birth showed a peak around postnatal day 5 (P5) (Fig. 1A), which coincided with the stage when cyclin E-CDK and cyclin A-CDK activities start to decrease [4]. $p57^{Kip2}$ was expressed strongly in midgestation (E12.5–14.5). The expression then decreased and could not

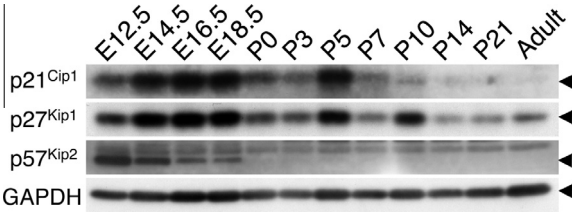

Fig. 1. Expression patterns of Cip/Kip family proteins during cardiac development. Cardiac ventricles at indicated developmental stages were analyzed by Western blot analysis. Arrowheads show the positions of positive signals.

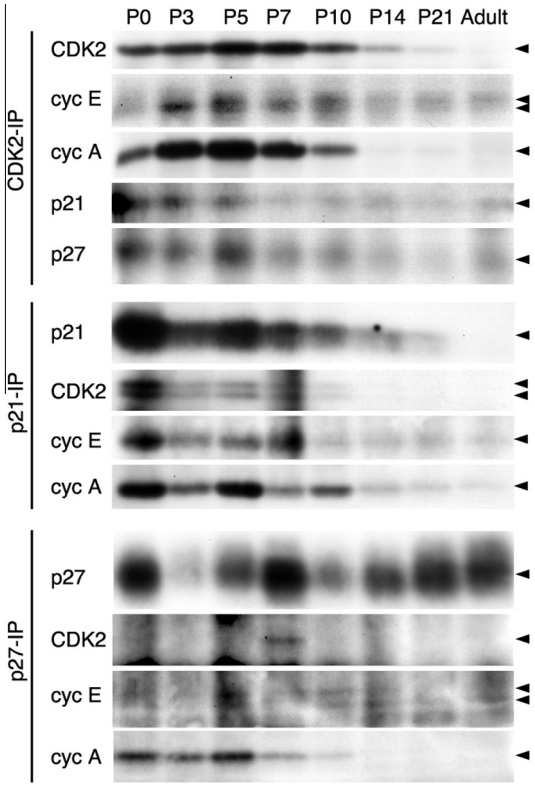

Fig. 2. Complex formation of $p21^{Cip1}$ and $p27^{Kip1}$ with cyclins and CDKs. Complex formation of $p21^{Cip1}$ and $p27^{Kip1}$ with cyclin E, cyclin A and CDK2. CDK2, $p21^{Cip1}$ and $p27^{Kip1}$ were immunoprecipitated with corresponding antibodies from the wild type cardiac ventricles indicated stages (CDK2-IP, p21-IP and p27-IP). Protein patterns of the complexes were analyzed by Western blot analysis. Arrowheads show the positions of positive signals.

be detected after birth (Fig. 1). Therefore, we focused on $p21^{Cip1}$ and $p27^{Kip1}$ in the subsequent studies.

Next, we examined the interaction between the two CKIs and CDK2 or the two CKIs and cyclins using immunoprecipitation (Fig. 2). Immunoprecipitation of CDK2 showed that CDK2 bound to $p21^{Cip1}$ and $p27^{Kip1}$ as well as cyclin E and cyclin A at postnatal stages (Fig. 2, CDK2-IP). On the contrary, $p21^{Cip1}$ and $p27^{Kip1}$bound to CDK2 as well as cyclin E and cyclin A (Fig. 2, p21-IP and p27-IP). Because the association of $p21^{Cip1}$ and $p27^{Kip1}$ with CDKs is greatly enhanced by cyclin binding [17], these data suggested that $p21^{Cip1}$ and $p27^{Kip1}$ bind to cyclin E-CDK2 or cyclin A-CDK2 complexes in postnatal cardiac ventricles.

3.2. Functions of $p21^{Cip1}$ and $p27^{Kip1}$ in cell cycle exit of CMs

We analyzed *$p21^{Cip1}$* and *$p27^{Kip1}$* KO mice to examine whether $p21^{Cip1}$ and $p27^{Kip1}$ are involved in the cell cycle exit of CMs. The external morphology and sizes of the hearts of *$p21^{Cip1}$* and *$p27^{Kip1}$* KO mice did not show any apparent differences when compared with those of control mice. In addition, the heart weight did not show any significant changes, although that of *$p27^{Kip1}$* KO mice in-

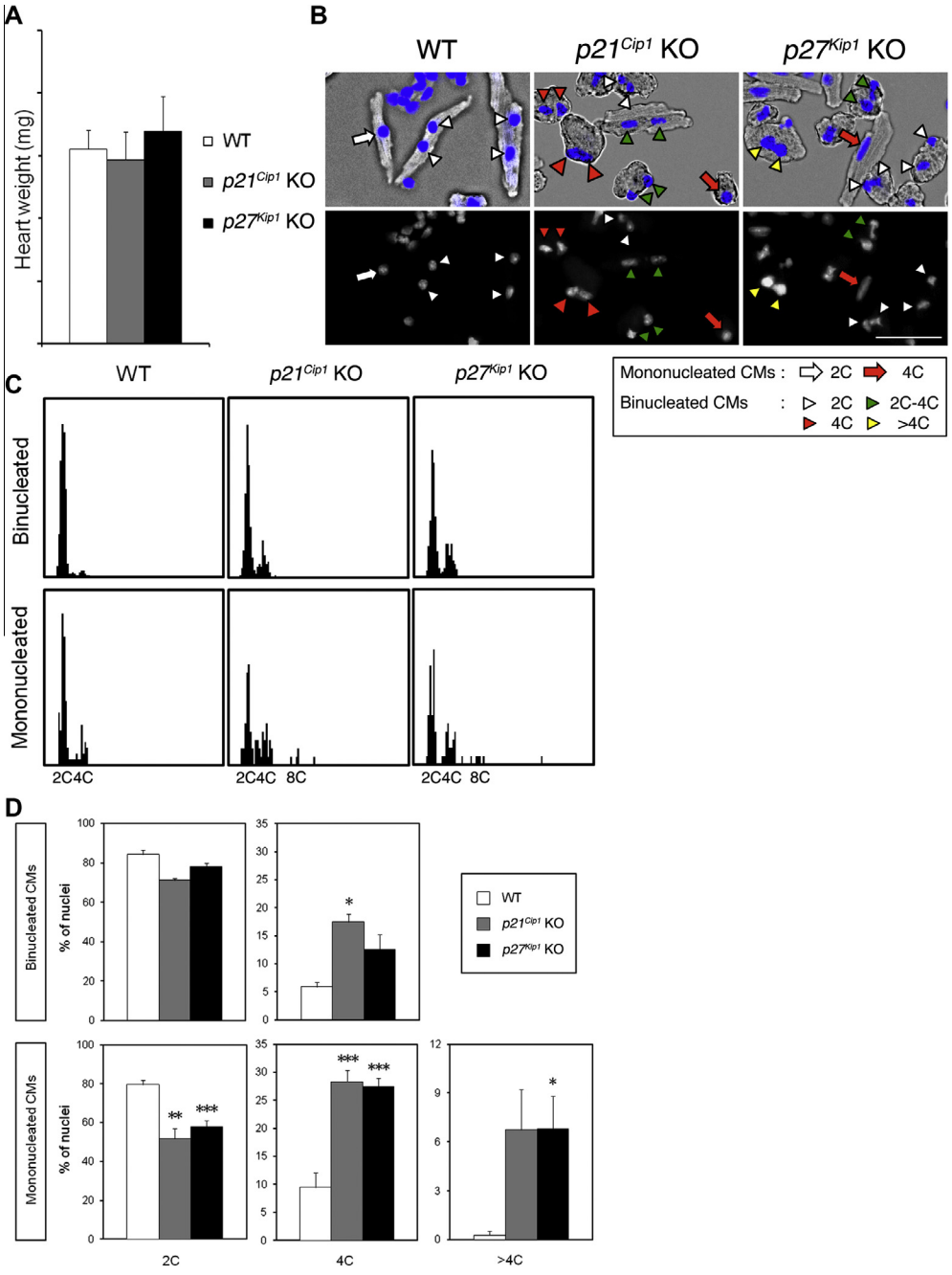

Fig. 3. Abnormal cell cycle exit in CMs of *$p21^{Cip1}$* and *$p27^{Kip1}$* KO mice. (A) Heart weight (mg) of wild type (WT), *$p21^{Cip1}$* KO, and *$p27^{Kip1}$* KO mice at P14 is presented as the mean + SE ($N = 3$). The differences were not statistically significant. (B) Examples of single CMs dissociated from ventricles of wild type, *$p21^{Cip1}$* KO and *$p27^{Kip1}$* KO mice at P14. Images stained with DAPI (lower panels) were merged with bright field images (upper panels). DAPI signals are shown in blue. Arrowheads and arrows represent various DNA contents (2C, 2C–4C, 4C or >4C) in nuclei of mono- and binucleated CMs, which were determined by measurement of DAPI fluorescence intensity. Scale bar, 50 μm. (C) Representative histograms showing the cell cycle distribution patterns of bi-(upper) and mononucleated (lower) CMs from the ventricles of control, *$p21^{Cip1}$* KO and *$p27^{Kip1}$* KO mice at P14. (D) Percentages of 2C, 4C and >4C nuclei in the cell cycle distribution patterns of bi- and mononucleated CMs at P14. Percentages are presented as the mean + SE ($N = 4$). $^{*}P < 0.05$; $^{**}P < 0.01$; $^{***}P < 0.005$ vs. wild type mice (Student's t test).

creased slightly (Fig. 3A). The results were consistent to the previous report [10].

Next, we analyzed the cell cycle distribution patterns of CMs in these KO mice using microphotometry, which is an established method [4]. We measured the DNA content per nucleus of a single CM dissociated from the ventricles on slide glasses, because FACS analysis can neither measure the DNA content in each nucleus in binucleated CMs nor distinguish between mono- and binucleated CMs. Nuclei with 2C, 2C–4C and 4C were regarded as those in G1, S and G2/M-phase, respectively.

The deficiency of $p21^{Cip1}$ or $p27^{Kip1}$ caused significant abnormalities in the cell cycle distribution patterns of CMs at P14, when the cell cycles of almost all CMs exited in wild type mice [3,4]. The mean percentages of 2C and 4C nuclei in binucleated CMs in control mice were 84.4% and 5.9%, respectively (Fig. 3D). These data are consistent with our previous study showing that almost of all binucleated CMs exit the cell cycle at the G1-phase after binucleation [4]. In contrast to control mice, the 2C population decreased slightly, and the 4C population increased in binucleated CMs of both KO mice (Fig. 3B–D). M-phase marker, pH3-S10 positive CMs were very rare or not observed in the 4C population (mean in *p21*^{Cip1} KO mice, 0.3%; *p27*^{Kip1} KO mice, 0%), indicating that almost all CMs in the population were at G2-phase. These results suggested that some nuclei of the binucleated CMs (*p21*^{Cip1} KO, 84.4–71.2 = 13.2%; *p27*^{Kip1} KO, 84.4–78.0 = 6.4%) did not exit the cell cycles at the G1-phase but rather proceeded to S- and then G2-phases.

The mean percentages of 2C and 4C in mononucleated CMs of control were 79.5% and 9.5%, respectively (Fig. 3D). These data are also consistent with our previous findings [4]. Mononucleated CMs with 2C decreased significantly in both KO mice. On the other hand, cells with 4C increased significantly (Fig. 3B–D). Most strikingly, >4C population including 8C, which was very rare in the control mice (mean, 0.3%), increased markedly in both KO mice (Fig. 3B–D, *p21*^{Cip1} KO, 6.8%; *p27*^{Kip1} KO, 6.8%). These results suggested that a portion of the mononucleated CMs did not exit the cell cycle at the G1-phase (at least, *p21*^{Cip1} KO, 79.5–51.8 = 27.7%; *p27*^{Kip1} KO, 79.5–57.7 = 21.8%) but proceeded to the S- and G2/M phases. In addition, some of the mononucleated CMs at the G2/M-phase, including cells which proceeded from the G1-phase, entered endoreplication.

We analyzed the cell cycle distribution patterns of *p21*^{Cip1} KO mice at P28, and almost similar results were obtained. In addition, the patterns of *p21*^{Cip1} KO mice at P0 and P5 did not show apparent abnormalities (data not shown). These data suggested that failure in the cell cycle exit at G1-phase occurred mainly between P5 and P14, and the cell cycle of these cells was arrested at the G2/M-phase (4C) or after endoreplication (>4C).

We also examined the percentages of EdU positive CMs in dissociated cells at P14. The percentages were extremely low in wild type mice (both bi- and mononucleated CMs, 0.3%), indicating cell cycle exit. However, these percentages increased markedly in both bi- and mononucleated CMs of p21 and p27 KO mice (Supplementarl Fig. 1), showing entry to S-phase, and failed cell cycle exit.

These data showed that $p21^{Cip1}$ and $p27^{Kip1}$ are strongly involved in cell cycle exit in both bi- and mononucleated CMs.

4. Discussion

In the present study, we showed the first apparent phenotypes in the hearts of Cip/Kip KO mice. No apparent abnormalities have been reported (see Section 1). Our data also suggest that $p21^{Cip1}$ and $p27^{Kip1}$ are critical factors for cell cycle exit of CMs in postnatal stages.

The cell cycle exit occurs at G1-phase (2C) in almost all bi- and mononucleated CMs of control mice (Fig. 3) [4]. While, the cell cycle was not arrested, and proceeded to G2-phase (4C) in a population of binucleated CMs of *p21*^{Cip1} and *p27*^{Kip1} KO mice (Fig. 3). The cell cycle of a population of mononucleated CMs proceeded to G2-phase, and then entered endoreplication (>4C) (Fig. 3). In both CMs, the percentages of EdU positive CMs increased markedly (Supplemental Fig. 1), indicating further progression of the cell cycle from G1-phase. These data showed that the cell cycle exit at G1-phase was inhibited in a population of CMs of *p21*^{Cip1} and *p27*^{Kip1} KO mice, and that $p21^{Cip1}$ and $p27^{Kip1}$ are involved in the cell cycle exit at G1-phase.

However, the cell cycle of these abnormal CMs (the 4C population in binucleated CMs, and >4C populations in mononucleated CMs) was arrested at G2-phase or entered endoreplication (Fig. 3). These data suggest that entry to M-phase was inhibited, and that mouse CMs have an inhibitory system, independent of $p21^{Cip1}$ and $p27^{Kip1}$, to maintain cell cycle exit. Interestingly, we observed similar phenotypes in cyclin D1-induced adult CMs (unpublished data).

Affected populations of CMs in *p21*^{Cip1} and *p27*^{Kip1} KO mice were relatively limited. Most likely, $p21^{Cip1}$ and $p27^{Kip1}$ have overlapping functions with each other. In fact, double KO of both genes enhanced their phenotypes in tumorigenesis [18]. Therefore, analysis of hearts in double KO mice will be helpful to examine the overlapping functions of $p21^{Cip1}$ and $p27^{Kip1}$ in the hearts. In addition, the analysis will show how factors other than $p21^{Cip1}$ and $p27^{Kip1}$ contribute to the cell cycle exit of CMs.

Our previous data suggested that unknown factor(s) inhibit the activities of cyclin E- and A-CDKs and that the inhibition is involved in the cell cycle exit of CMs in postnatal stages [4]. Expression patterns during postnatal stages and phenotypes of KO mice in the cell cycle exit suggested that $p21^{Cip1}$ and $p27^{Kip1}$ are at least two of the unknown factors. If this is the case, the activities of cyclin E- and A-CDKs might not decrease in affected CMs at P5. However, their detection would be impossible because the affected populations are limited in *p21*^{Cip1} or *p27*^{Kip1} KO mice. It is therefore probably more appropriate to consider the issue in double KO mice.

It is very interesting how transient expression of $p21^{Cip1}$ and $p27^{Kip1}$ is controlled in postnatal CMs. A recent report shows that Meis1 acts as a transcriptional repressor of *p21*^{Cip1} in postnatal CMs [19]. However, detailed molecular mechanisms of Meis1 for *p21*^{Cip1}, and an upstream system for $p27^{Kip1}$ in CMs, are still unknown.

Elucidation of these issues above will provide new insights to regulation of CMs proliferation and will contribute to regenerative therapy by the proliferation of pre-existing CMs.

Acknowledgments

The authors wish to thank Dr. Philip Leder (Harvard Medical School, Boston) for kindly providing the *p21*^{Cip1} knockout mice. We also thank Ms. Satomi Ikuta (Tottori University, Yonago) for her technical assistance. This work was partially supported by a research Grant from the Ministry of Education, Culture, Sports, Science and Technology of Japan.

Appendix A. Supplementary data

Supplementary data associated with this article can be found, in the online version, at http://dx.doi.org/10.1016/j.bbrc.2013.12.109.

References

[1] I.L. Erokhina, Proliferation dynamics of cellular elements in the differentiating mouse myocardium, Tsitologia 10 (1968) 1391–1409.
[2] M. Toyoda, H. Shirato, K. Nakajima, M. Kojima, M. Takahashi, M. Kubota, R. Suzuki-Migishima, Y. Motegi, M. Yokoyama, T. Takeuchi, Jumonji downregulates cardiac cell proliferation by repressing cyclin D1 expression, Dev. Cell 5 (2003) 85–97.
[3] M.H. Soonpaa, K.K. Kim, L. Pajak, M. Franklin, L.J. Field, Cardiomyocyte DNA synthesis and binucleation during murine development, Am. J. Physiol. 271 (1996) H2183–H2189.
[4] A. Ikenishi, H. Okayama, N. Iwamoto, S. Yoshitome, S. Tane, K. Nakamura, T. Obayashi, T. Hayashi, T. Takeuchi, Cell cycle regulation in mouse heart during embryonic and postnatal stages, Dev. Growth Differ. 54 (2012) 731–738.
[5] M. Mollova, K. Bersell, S. Walsh, J. Savla, L.T. Das, S.-Y. Park, L.E. Silberstein, C.G. dos Remedios, D. Graham, S. Colan, B. Kuhn, Cardiomyocyte proliferation contributes to heart growth in young humans, Proc. Natl. Acad. Sci. 110 (2013) 1446–1451.
[6] S.E. Senyo, M.L. Steinhauser, C.L. Pizzimenti, V.K. Yang, L. Cai, M. Wang, T.-D. Wu, J.-L. Guerquin-Kern, C.P. Lechene, R.T. Lee, Mammalian heart renewal by pre-existing cardiomyocytes, Nature 493 (2013) 433–436.
[7] C.J. Sherr, J.M. Roberts, CDK inhibitors: positive and negative regulators of G1-phase progression, Genes Dev. 13 (1999) 1501–1512.
[8] C. Deng, P. Zhang, J. Wade Harper, S.J. Elledge, P. Leder, Mice lacking p21Cip1/Waf1 undergo normal development, but are defective in G1 checkpoint control, Cell 82 (1995) 675–684.
[9] J. Brugarolas, C. Chandrasekaran, J.I. Gordon, D. Beach, T. Jacks, G.J. Hannon, Radiation-induced cell cycle arrest compromised by p21 deficiency, Nature 377 (1995) 552–557.
[10] H. Kiyokawa, R.D. Kineman, K.O. Manova-Todorova, V.C. Soares, E.S. Hoffman, M. Ono, D. Khanam, A.C. Hayday, L.A. Frohman, A. Koff, Enhanced growth of mice lacking the cyclin-dependent kinase inhibitor function of p27Kip1, Cell 85 (1996) 721–732.
[11] K. Nakayama, N. Ishida, M. Shirane, A. Inomata, T. Inoue, N. Shishido, I. Horii, D.Y. Loh, K.-I. Nakayama, Mice lacking p27Kip1 display increased body size, multiple organ hyperplasia, retinal dysplasia, and pituitary tumors, Cell 85 (1996) 707–720.
[12] Y. Yan, J. Frisen, M.H. Lee, J. Massague, M. Barbacid, Ablation of the CDK inhibitor p57Kip2 results in increased apoptosis and delayed differentiation during mouse development, Genes Dev. 11 (1997) 973–983.
[13] K. Takahashi, K.-I. Nakayama, K. Nakayama, Mice lacking a CDK inhibitor, p57Kip2, exhibit skeletal abnormalities and growth retardation, J. Biochem. 127 (2000) 73–83.
[14] T. Shioya, A simple technique for isolating healthy heart cells from mouse models, J. Physiol. Sci. 57 (2007) 327–335.
[15] K. Nakajima, M. Inagawa, C. Uchida, K. Okada, S. Tane, M. Kojima, M. Kubota, M. Noda, S. Ogawa, H. Shirato, M. Sato, R. Suzuki-Migishima, T. Hino, Y. Satoh, M. Kitagawa, T. Takeuchi, Coordinated regulation of differentiation and proliferation of embryonic cardiomyocytes by a jumonji (jarid2)-cyclin D1 pathway, Development 138 (2011) 1771–1782.
[16] H. Shirato, S. Ogawa, K. Nakajima, M. Inagawa, M. Kojima, M. Tachibana, Y. Shinkai, T. Takeuchi, A jumonji (jarid2) protein complex represses cyclin D1 expression by methylation of histone H3–K9, J. Biol. Chem. 284 (2009) 733–739.
[17] J.W. Harper, S.J. Elledge, K. Keyomarsi, B. Dynlacht, L.H. Tsai, P. Zhang, S. Dobrowolski, C. Bai, L. Connell-Crowley, E. Swindell, Inhibition of cyclin-dependent kinases by p21, Mol. Biol. Cell 6 (1995) 387–400.
[18] R.A. Garcia-Fernandez, P. Garcia-Palencia, M.A. Sanchez, G. Gil-Gomez, B. Sanchez, E. Rollan, J. Martin-Caballero, J.M. Flores, Combined loss of p21Waf1/Cip1 and p27Kip1 enhances tumorigenesis in mice, Lab. Invest. 91 (2011) 1634–1642.
[19] A.I. Mahmoud, F. Kocabas, S.A. Muralidhar, W. Kimura, A.S. Koura, S. Thet, E.R. Porrello, H.A. Sadek, Meis1 regulates postnatal cardiomyocyte cell cycle arrest, Nature 497 (2013) 249–253.